The paper was published in the proceedings of the 11th International Conference on Scour and Erosion and was edited by Thor Ugelvig Petersen and Shinji Sassa. The conference was held in Copenhagen, Denmark from September 17th to September 21st 2023.

Assessment of Scour Hazard Risk Around Bridge Piers—Framework and Case Study

Chao Huang,[1] Nasi Zhang,[2] Haoyin Shan,[3] James Pagenkopf,[4] and Kornel Kerenyi[5]

[1]Genex Systems, Turner-Fairbank Highway Research Center (TFHRC) Hydraulics Research Laboratory, 6300 Georgetown Pike, McLean, VA 22101, USA; e-mail: c.huang.ctr@dot.gov, Corresponding author
[2]Genex Systems, TFHRC Hydraulics Research Laboratory, 6300 Georgetown Pike, McLean, VA 22101, USA; e-mail: nasi.zhang.ctr@dot.gov
[3]Genex Systems, TFHRC Hydraulics Research Laboratory, 6300 Georgetown Pike, McLean, VA 22101, USA; e-mail: haoyin.shan.ctr@dot.gov
[4]Federal Highway Administration (FHWA), TFHRC Hydraulics Research Laboratory, 6300 Georgetown Pike, McLean, VA 22101, USA; e-mail: james.pagenkopf@dot.gov
[5]FHWA, TFHRC Hydraulics Research Laboratory, 6300 Georgetown Pike, McLean, VA 22101, USA; e-mail: kornel.kerenyi@dot.gov

ABSTRACT

Over the past few decades, more than 47 percent of bridge failures in the United States were caused by scour and/or hydraulic issues. This paper presents a framework to assess the exceedance probability for incremental scour depths (i.e., scour hazard risk) in bridge foundation design through a probabilistic analysis. The natural uncertainty, hydrological modeling uncertainty, hydraulic modeling uncertainty, equation uncertainty, and the uncertainty of the soil's critical shear stress were considered to develop the hydraulic load and resistance distributions. Decay functions were used to relate presumed scour depths to bed shear stresses. A Monte Carlo simulation was performed to realize the combination of uncertainties in load and resistance to obtain the exceedance probability of scour at various elevations at the foundation. A case study of the Lafayette Avenue Bridge replacement project in Michigan demonstrates the procedure of assessing the scour hazard risk level using the framework. The obtained scour hazard risk can potentially be incorporated with Load and Resistance Factor Design (LRFD) Bridge Design Specifications (BDS) under a consistent risk-based frame.

INTRODUCTION

Highway bridges are essential components of the transportation infrastructure. Any failure can cause significant damage and result in traffic disruptions that lead to enormous direct and indirect losses in the affected area. According to a statistical analysis of bridge failures in the United States, over the past three decades, scour and hydraulic issues caused more than 47 percent of failures in existing bridges (Lee et al. 2013).

Current design guidelines and specifications address the risk of scour-related foundation and structural failure by including a predicted scour depth in the foundation design. For shallow foundations, once the footing is undermined by a scour hole, the vertical support to the foundation will reduce dramatically, potentially leading to the failure of the bridge foundation. In considering the loss of bearing capacity caused by the amount of scour, current practices of deep foundations require driving the piles to a sufficient depth to provide needed resistance. In general, the scour equations are conservative in offering a significant margin of safety. However, these equations are not formulated and calibrated in a framework consistent with the American Association of State Highway and Transportation Officials (AASHTO) Load and Resistance Factor Design (LRFD) Bridge Design Specifications (BDS) practice of probability-based bridge design. (AASHTO 2020).

This paper proposes a framework to estimate the probability of exceedance of scour for incremental scour depths. The natural uncertainty, hydrological modeling uncertainty, hydraulic modeling uncertainty, and equation uncertainty were considered when developing the load distribution. A decay function was adopted to calculate the riverbed shear stress for the incremental scour depths (Kerenyi and Flora 2019). The uncertainties of the critical shear stress of soil were considered when developing the resistance distribution. A Monte Carlo simulation was performed to realize the combination of the uncertainties in load and resistance. Probability of exceedance (or exceedance probability) of scour for the incremental scour depths, $P_{e,scour}$, was calculated. As a result, the relationship between $P_{e,scour}$ and the corresponding scour depth was finally obtained and presented. A probabilistic analysis of scour calculations is a central aspect of FHWA's next generation of scour design methodology, NextScour (FHWA 2023).

NextScour Case Study: The Lafayette Avenue Bridge over the Saginaw River in Bay City, Michigan demonstrates the procedure of assessing the scour hazard risk level using the framework (FHWA 2023). The obtained scour hazard risk can potentially be incorporated with LRFD BDS under a consistent risk-based frame.

CONCEPT OF LOAD AND RESISTANCE IN SCOUR DESIGN

In the current AASHTO LRFD BDS, load and resistance generally refer to the forces applied on a bridge structure by internal or external sources and the capability of the designed structure to resist such forces, respectively (AASHTO 2020). In the historical development of LRFD BDS, load and resistance distributions were investigated and compared using the derived design limit state equations to ensure the reliability of bridge structures remains at a consistent level.

When the concept is applied to the scour hazard, the load can be deemed as the riverbed bed shear stress produced by the flow, and the resistance can be deemed as the critical shear stress of the soil. When the flow-induced bed shear stress exceeds the critical shear stress of the soil, scour results. $P_{e,scour}$ represents the probability of the actual scour exceeding a certain scour depth, where scour depth is y_s. Figure 1 shows conceptual load (L) and resistance (R) distribution in terms of probability density functions (PDF) and $P_{e,scour}$ for a specific scour depth. The distribution of the load, τ_b, is calculated from a Monte Carlo simulation considering various uncertainties of flood events. The distribution of the resistance, τ_c, is obtained from soil erosion tests. The shaded area represents $P_{e,scour}$.

When $P_{e,scour}$ is calculated for incremental scour depths, a relationship between $P_{e,scour}$ and scour depth is established, as shown in Figure 2. The detailed procedure for the proposed approach will be discussed in the following sections.

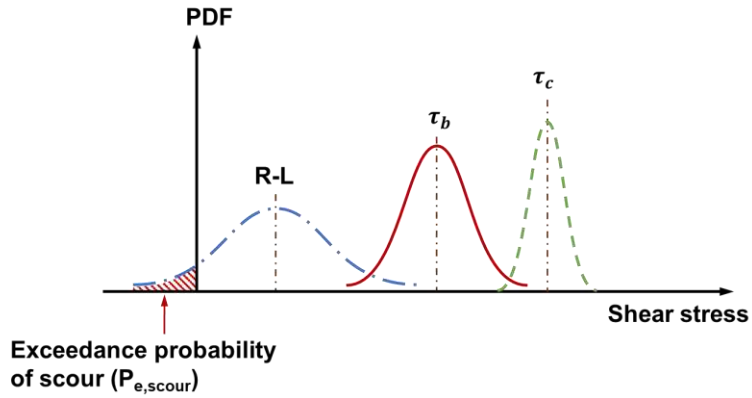

Source: FHWA.

Figure 1. Load distribution, resistance distribution, and $P_{e,scour}$.

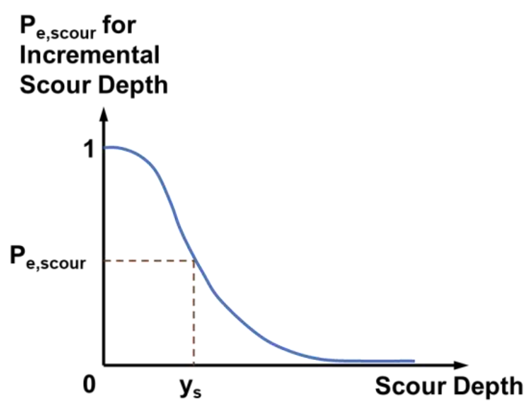

Source: FHWA.

Figure 2. Relationship of $P_{e,scour}$ versus scour depth.

LOAD DISTRIBUTION

The hydraulic load distribution (the distribution of bed shear stress resulting from stream flow) is calculated by considering various sources of uncertainties, including the natural uncertainty, hydrological modeling uncertainty, hydraulic modeling uncertainty, and equation uncertainty (Huang, Kerenyi, and Shen 2019).

Natural uncertainty. The current AASHTO LRFD BDS specifies the design flood for bridge scour to be the flood flow equal to or less than the design flood with a return period of 100 yr (Q_{100}) that creates the deepest scour at bridge foundations (AASHTO 2020). In practice, during the design life of a bridge structure (i.e., 75 yr), a bridge may experience floods of any return period, and it is not trivial to determine the actual peak flood. Therefore, the full spectrum of flooding with various discharges must be taken into consideration instead of a few deterministic discharges, such as Q_{100} or Q_{500}. In this case, the natural uncertainty is considered by randomly generating 75 exceedance probabilities (P_e) between 0 and 1 for the annual peak discharge, which is equivalent to generating one individual P_e for each year in the bridge design life.

Hydrological modeling uncertainty. Based on Beard's flood event studies and Bulletin 17C of the Advisory Committee on Water Information, a log-Pearson Type III (LPIII) distribution was selected to describe the frequency of annual peak floods (Beard 1974; England et al. 2019). The uncertainties introduced by the parameters of the LPIII distribution model were considered as the hydrological modeling uncertainty.

Hydraulic modeling uncertainty. Theoretical and numerical hydraulic models are used to calculate the flow conditions, such as flow depths, flow velocities, and bed shear, for a given river bathymetry and bridge structure geometry. This research considered the uncertainties of hydraulic models and the hydraulic input.

Equation uncertainty: uncertainty on hydraulic loading decay function for bridge structures. The most widely used scour design guideline in the United States, *Hydraulic Engineering Circular No. 18* (HEC-18), addresses the scour design by predicting a deterministic scour depth (Arneson et al. 2012). HEC-18 has implicitly implemented the hydraulic loading decay function concepts in various sections. The decay trend of the riverbed bed shear stress with increasing scour depth attributes to the reduced flow velocity and strength of vortices when the scour hole progresses around bridge structures. This phenomenon can be observed in almost all experiments and practices. FHWA has expanded the research (e.g., Annandale 2005), proposing decay functions for various scour components to calculate the bed shear stress from the scour depth and comparing them with the critical shear stress to obtain a more accurate scour depth prediction.

Decay functions for pier scour can be developed using a bootstrapping approach and least squares regression for experimental studies and/or computational fluid dynamics (CFD) simulations (Efron and Tibshirani 1994). Figure 3 contains the experimental results from Annandale's study and FHWA CFD simulations (Annandale 2005; Shan et al. 2023). Figure 3 shows an example decay relationship between the ratio of shear stress near the pier to approach shear stress (τ_{pier}/τ_a) and the ratio of incremental scour depths to projected pier width ($y_{s,pier}/a_{proj}$). The decay function in the form of Eq. 1 was adopted. Constants a and b are determined through linear regression on the logarithm form of Eq. 1:

$$\frac{\tau_{pier}}{\tau_a} = a \times e^{b \times \frac{y_{s,pier}}{a_{proj}}} \tag{1}$$

where τ_{pier} (lb/ft^2, Pa) is the bed shear stress at the pier, $y_{s,pier}$ (ft, m) is the pier scour depth, and a_{proj} (ft, m) is the projected pier width calculated by Eq. 2:

$$a_{proj} = w \cdot cos\,\theta + l \cdot sin\,\theta \tag{2}$$

where w (ft, m) is the pier width, l (ft, m) is the pier length, and θ is the flow angle of attack in degrees. τ_a (lb/ft^2, Pa) is calculated by Eq. 3:

$$\tau_a = \gamma_w \frac{(V_1 n)^2}{y_1^{1/3} K_u^2} \tag{3}$$

where γ_w (lb/ft^3, N/m^3) is the unit weight of water, n is Manning's roughness coefficient, V_1 (ft/s, m/s) is the approach flow velocity in the main channel, K_u is 1.486 in English units and 1.0 for International System (SI) units, and y_1 (ft, m) is the flow depth upstream of the bridge.

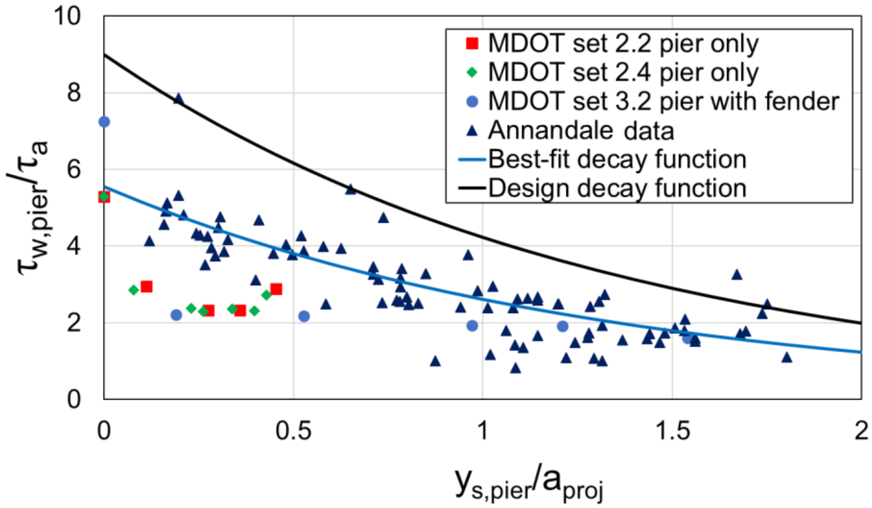

Source: FHWA.
MDOT = Michigan Department of Transportation.

Figure 3. Graph. General decay function for pier scour.

RESISTANCE DISTRIBUTION

In this study, critical shear stress of the soil is considered as the only resistance to scour hazard. Critical shear stress can be obtained from In-situ Scour Testing Device (ISTD) tests, Ex-situ Scour Testing Device (ESTD) tests, or Portable Scour Testing Device (PSTD) tests on the soil samples. The uncertainty of the soil's critical shear stress results in the resistance distribution. FHWA described two methods to generate the soil resistance distribution, including the bin method and the bootstrapping method, and the results are used in this study (FHWA 2023). The bootstrapping method was applied in determining the distribution of critical shear stress from the soil erosion test results.

MONTE CARLO SIMULATION FOR PROBABILISTIC SCOUR ANALYSIS

Monte Carlo simulation is a powerful tool to predict the probability of an output parameter when considering various input parameters as random variables (Doucet, Freitas, and Gordon 2001). In an m-point Monte Carlo simulation, a total of m random values is generated for each variable according to its statistical properties, thereby generating m sets of input parameters. The result is m outcomes obtained from the m sets of input parameters. If m is sufficiently large, the statistical properties of the results will approximate the actual properties of the event. Figure 4 shows a flowchart illustrating the steps to perform an m-point Monte Carlo simulation for probability scour analysis, considering the uncertainties in load and resistance distributions. The statistical parameters are defined as follows: sample mean ($\bar{X}$), sample standard deviation (S), sample skewness (G), population mean (μ), population standard deviation, (σ), population skewness (γ).

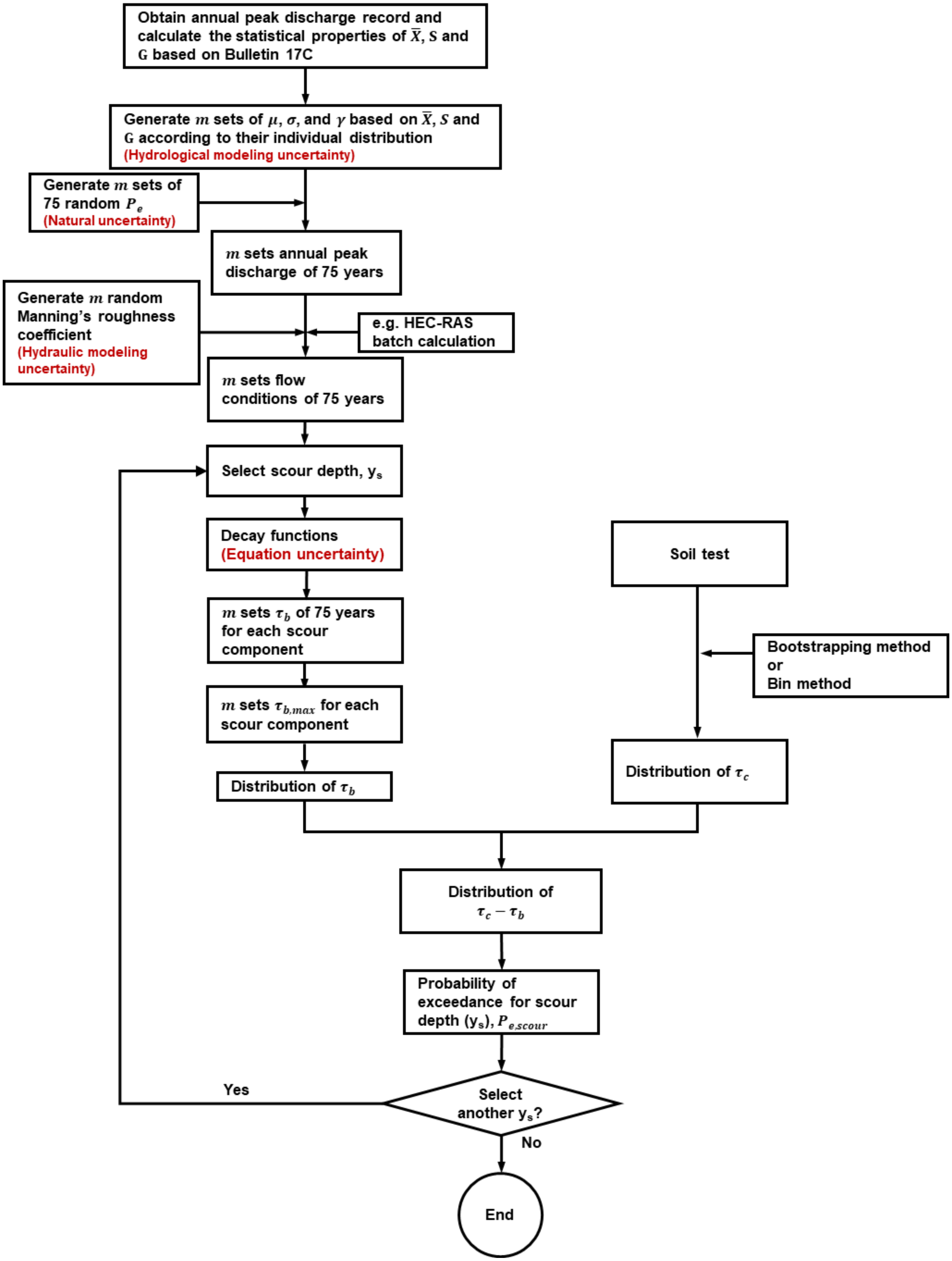

Source: FHWA.

Figure 4. Monte Carlo simulation on probability scour analysis.

This simulation includes the following steps:

Step 1: Generate annual maximum discharge for the design life of the bridge. If an m- point Monte Carlo simulation is performed on a bridge with a 75-yr design life, $75 \cdot m$ annual maximum discharges should be generated.

1. Obtain the historical maximum annual discharges information ($Q_1, \ldots, Q_N$) from available resources. Next, calculate the sample and population statistical properties according to *Bulletin 17C*.
2. Randomly select m sets of population statistics from the distribution curves.
3. Randomly select 75 exceedance probabilities ($P_{e,(i,j)}$) for each set of μ_i, σ_i, and γ_i. Here, 75 represents the 75-yr design life of a bridge. j represents the jth year of the bridge design life, where $j = 1, 2, \ldots, 75$. The symbol (i, j) indicates the jth year of bridge life for the ith dataset in the Monte Carlo simulation.
4. Calculate the annual peak discharge $Q_{(i,j)}$ for each year in bridge design life for each set of Monte Carlo simulation parameters.

Step 2: Generate Manning's roughness *n*. For an m-point Monte Carlo simulation, m sets of Manning roughness n are generated, with the assumption that Manning n does not change during the bridge's design life.

Step 3: Compute the flow conditions. Submit $Q_{(i,j)}$ ($i = 1, 2, \ldots, m$ and $j = 1, 2, \ldots, 75$) and n_i to a hydraulic model (e.g., HEC-RAS model), and compute the flow conditions, including flow velocity, flow depth, and unit discharge, etc.[1] Eventually, $75 \cdot m$ sets of flow conditions are calculated for determining the load distribution (the distribution of τ_b) in step 5.

Step 4: Select the scour depth series. The incremental scour depths, $y_{s,1}, y_{s,2}, \ldots, y_{s,t}$, are selected by the designers or bridge owners according to their interests. The load distribution (distribution of τ_b) and resistance distribution (distribution of τ_c) are calculated and generated for each scour depth $y_{s,k}$, where $k = 1, 2, \ldots, t$. $P_{e,scour}$ values are calculated for the selected scour depth series.

Step 5: Determine the load distribution, i.e., the distribution of bed shear stress (τ_b). The distribution of τ_b is calculated for different scour components. The procedure of obtaining the distribution of τ_{pier} is shown as follows:

1. Generate m set of coefficients a and b in Eq. 1.
2. Select one scour depth from the incremental scour depth series, e.g., $y_{s,1}$.
3. Input $y_{s,1}$, $75 \cdot m$ sets of flow conditions, and m sets of n, a, and b to Eqs. 1 and 3, resulting in $75 \cdot m$ sets of $\tau_{b,pier(i,j),1}$, where i is the ith data set in Monte Carlo simulation, j is the jth year of bridge life, and "1" is the first scour depth in the scour depth series.
4. Find the maximum bed shear stress for pier scour in the 75-yr bridge design life for every set of Monte Carlo simulation parameters, which results in m points of $\tau_{b,pier,max(i),1}$.

[1] https://www.hec.usace.army.mil/software/hec-ras/

5. The distributions of bed shear stress for pier scour at the selected scour depth ($y_{s,1}$) are obtained from the distribution of m points of $\tau_{b,pier,max(i),1}$.
6. Move to the next scour depth in the scour depth series, $y_{s,2}$. Repeat steps 2 and 6 until the distributions of maximum bed shear stress for pier scour are obtained for every scour depth (from $y_{s,1}$ to $y_{s,t}$) assessed.

Step 6: Determine the resistance distribution, i.e., the distribution of τ_c. ISTD, ESTD, or PSTD soil tests are commonly performed on the soil samples to obtain the critical shear stress as the resistance to erosion forces. The flow rate time series, eroded soil depth time series, and the shear stress time series are recorded in these tests. This study uses the results from previous research (FHWA 2023).

Step 7: Calculate $P_{e,scour}$ for each scour component at the incremental scour depths. With both load and resistance distributions known, the $P_{e,scour}$ at the selected scour depth series for each scour component are calculated by the probability of critical shear stress (τ_c) that is smaller than the corresponding bed shear stress (τ_w). Figure 2 is drawn for each scour component (i.e., contraction, abutment, pier, and total pier scour).

CASE STUDY: LAFAYETTE AVENUE BRIDGES IN MICHIGAN

The Lafayette Avenue Bridge in Bay City, MI, is a bascule bridge over the Saginaw River. Maintained by the Michigan Department of Transportation (MDOT), the bridge is currently under investigation for a replacement. The proposed bridge features two large bascule piers that create complex flow patterns due to their wide widths.

The probability scour analysis was performed on the proposed new bridge using a 10,000-point Monte Carlo simulation for 75-yr bridge design life. $P_{e,scour}$ for various scour components at the selected scour depth series was calculated following steps 1–7 detailed in the previous section. A comparison between $P_{e,scour}$ and the probability of flood exceedance of various flood levels was performed for a better understanding of the results. The HEC-RAS model for this project is shown in Figure 5.

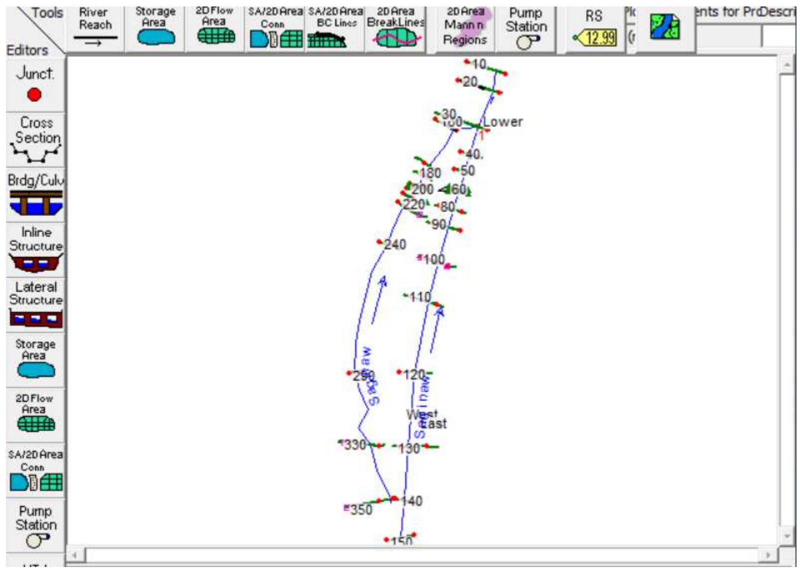

Source: FHWA.

Figure 5. HEC-RAS model for the Lafayette Avenue Bridge.

Step 1: Generate annual maximum discharge. The United States Geological Survey (USGS) gage 04157005 is about 12.5 mi upstream of the Lafayette Avenue Bridge. $\bar{X}$, S, and G for LPIII distribution were calculated using the peak floods provided in the HEC-RAS model. The regressed parameters were used to generate μ, σ, and γ. For the 10,000-point Monte Carlo simulation, 10,000 sets of parameters were generated. For each set, 75 exceedance probabilities ($P_{e,(i,j)}$, j = 1, 2, … 75) were randomly selected to represent every year of the 75-yr bridge design life. In total, 750,000 discharges were generated. Figure 6 shows the probability mass function (PMF) of the 750,000 annual peak discharges and the PMF of the 10,000 annual maximum discharges for every 75 years at the HEC-RAS model inlet.

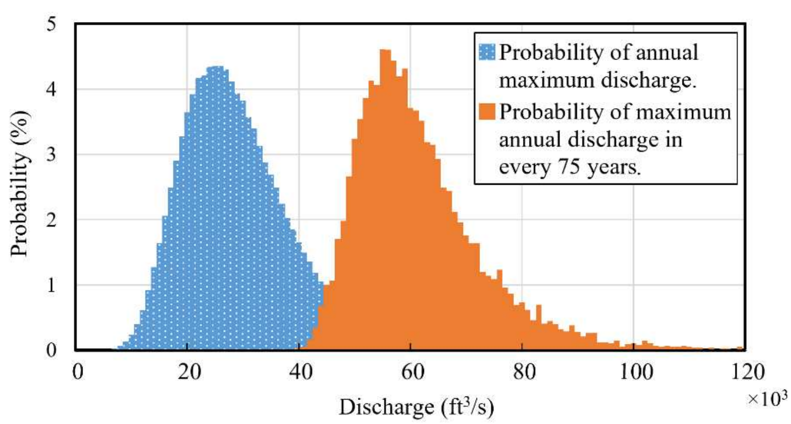

Source: FHWA.

Figure 6. PMF of annual maximum discharge and maximum annual discharge in every 75 yr for the Lafayette Avenue Bridge (FHWA 2023).

Step 2: Generate Manning roughness *n*. Manning's *n* is the only random variable considered in the hydraulic model uncertainty and is considered constant in the bridge design life. *NCHRP Report 761* indicates that Manning's *n* follows a lognormal distribution with a coefficient of variation (COV) of 0.015 (Lagasse et al. 2013). MDOT used 0.03 for the main channel and 0.08 for the overbanks in the HEC-RAS model. Figure 7 shows the PMF of generated Manning's *n* for the Saginaw River (FHWA 2023).

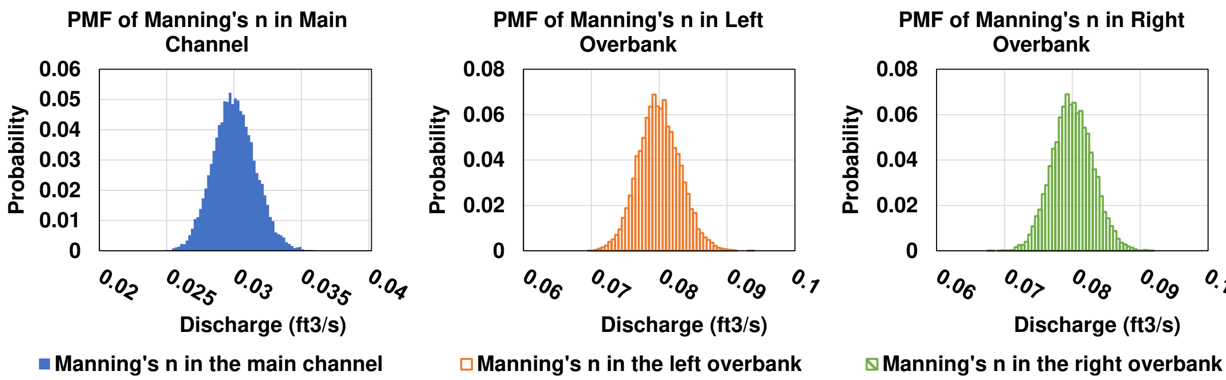

Source: FHWA.

Figure 7. PMF of generated Manning's *n* for the Saginaw River.

Step 3: Compute the flow conditions. 750,000 sets of discharges and 10,000 Manning's *n* were submitted to the revised HEC-RAS model via a batch job. A resulting 750,000 sets of flow conditions at the approach cross sections and the bridge cross section were obtained for calculating the bed shear stresses.

Step 4: Select the incremental scour elevation series. The selected scour elevations were 550, 540, 530, 520, and 510 ft for the total pier scour.

Step 5: Determine the distribution of bed shear stress (τ_b). For this project, specific decay functions were developed based on a series of flume tests with various configurations. For each test configuration, the incremental scour bathymetries were collected by an underwater laser scanner and then imported into three-dimensional (3D) CFD models to compute the nominal bed shear stress to develop the unique decay functions. Since the nominal shear stresses computed by the 3D CFD modeling have already included the shear from both pier scour and contraction scour effects, the decay function for pier scour developed herein comprises the total pier scour.

The bootstrapping method was used to develop the decay function (Efron and Tibshirani 1994). The best fit decay functions were determined as Eq. 1. The parameter $a = 7.14$ in Eq. 1 follows normal distributions with a COV of 0.48. The parameter $b = -0.81$ is a constant.

Since scour mainly occurs around the upstream fender cylinder, the projected width was taken as the fender diameter ($a_{proj} = 7.6$ m). The details to develop decay functions and the uncertainties can be found in previous research (FHWA 2023).

The modification factor for pier scour, $K_{m,pier}$, was determined by the ratio of the nominal shear stress obtained from the CFD simulations to the bed shear stresses calculated from Eq. 3 at various flood discharges when no scour occurs (i.e., at zero scour depth), and is presented as Eq. 4.

$$K_{m,pier} = 0.4F_r + 0.095 \quad (4)$$

where Fr is the Froude number calculated by Eq. 5:

$$F_r = \frac{V_1}{\sqrt{gy_1}} \quad (5)$$

where V_1 (ft/s, m/s) is the approach flow velocity; y_1 (ft, m) is the hydraulic depth at the approach cross section; and g (ft/s^2, m/s^2) is the acceleration of gravity.

For each scour elevation, 750,000 sets (10,000 sets for each 75-y bridge design life) of bed shear stresses for the total pier scour ($\tau_{b,total}$) were calculated using the HEC-RAS flow parameters and Eqs. 3 and 4. The load distribution was the distribution of the 10,000 maximum bed shear stresses. Figure 8 shows the PDF of the bed shear stresses at selected scour elevations.

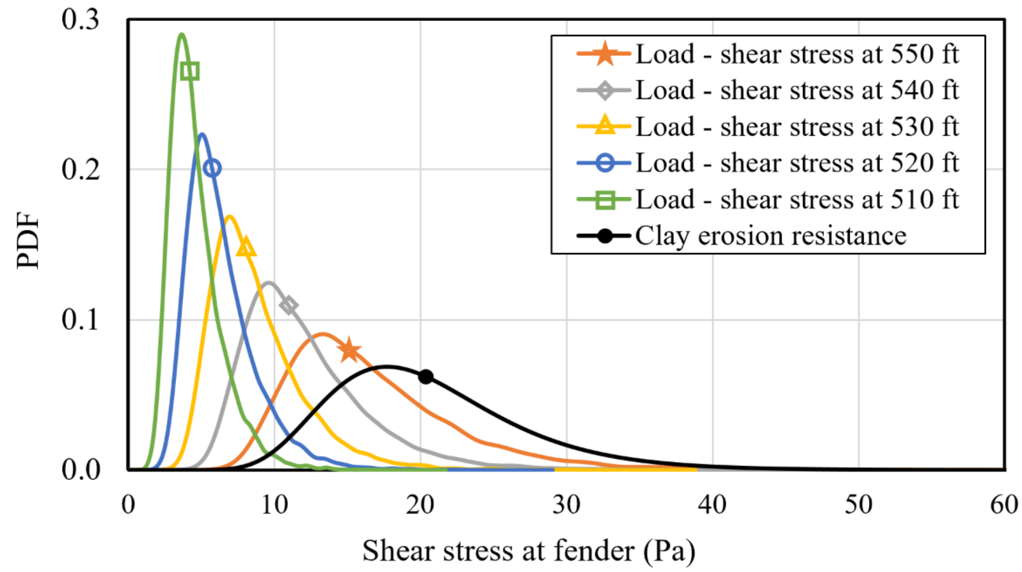

Source: FHWA.

Figure 8. Bed shear stress distribution for total pier scour (FHWA 2023).

Step 6: Determine the distribution of critical shear stress (τ_c). ESTD erosion tests were performed on soil samples with a duration of 10 min for each flow rate. A total of 1,127 erosion data points were collected. Using the bootstrapping approach, the mean value, standard deviation, and COV of the critical shear stress were calculated from 50,000 critical shear stresses to be 20.5 Pa (0.431 psf), 6.56 Pa (0.138 psf), and 0.32, respectively. Assuming the critical shear stress follows a lognormal distribution, the parameters for the lognormal distribution were calculated from the statistics used to generate the distribution, as shown in Figure 8.

Step 7: Calculate the $P_{e,scour}$ at the selected scour depth and scour elevation series. The load distribution (load-shear stress in Figure 8) were compared with the resistance distribution (clay erosion resistance in Figure 8). $P_{e,scour}$ was calculated as the probability of critical shear stress that was less than the bed shear stress. Figure 9 and Table 1 show $P_{e,scour}$ for total pier scour at various scour elevations. Note that the clay layer starts at the 530-ft elevation. Figure 9 indicates $P_{e,scour}$ at 530-ft is 3.3 percent.

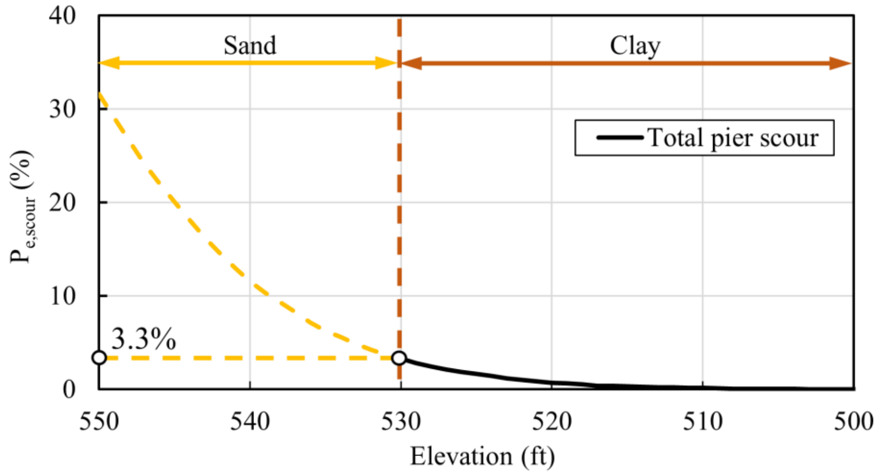

Source: FHWA.

Figure 9. $P_{e,scour}$ for total pier scour at various scour elevations (FHWA 2023).

Table 1. $P_{e,scour}$ for total pier scour at selected scour elevations.

Scour Depth (ft)	Scour Elevation (ft)	$P_{e,scour}$ for Total Pier Scour (%)
0	550	31.6
10	540	11.5
20	530	3.3
30	520	0.7
40	510	0.2

UNDERSTANDING $P_{E,SCOUR}$

Appendix B in HEC-18 emphasizes that for any flood design level, the design flood might be exceeded in any year (Arneson et al. 2012). This probability of exceedance increases with the life of the bridge. For example, for a Q_{100} flood, the annual probability of exceedance is 1/100, i.e., the probability of occurrence of a flood equal to or larger than Q_{100} is 1 percent in one year. When considering the bridge design life, the exceedance probability of Q_{100} is 52.9 percent in 75 yr.

Table 2 shows the probability of exceedance of various flood frequencies for different life spans of a bridge (N_{life}). For example, the $P_{e,scour}$ of Q_{200} for a 75-yr design life is 31.3 percent, and the $P_{e,scour}$ of Q_{500} for a 75-y design life is 13.9 percent.

Table 2. Probability of flood exceedance of various flood levels (Arneson et al. 2012).

Flood Frequency (yr)	N_{life} = 1 (%)	N_{life} = 5 (%)	N_{life} = 10 (%)	N_{life} = 25 (%)	N_{life} = 50 (%)	N_{life} = 75 (%)	N_{life} = 100 (%)
10	10.0	41.0	65.1	92.8	99.5	100.0	100.0
25	4.0	18.5	33.5	64.0	87.0	95.3	98.3
50	2.0	9.6	18.3	39.7	63.6	78.0	86.7
100	1.0	4.9	9.6	22.2	39.5	52.9	63.4
200	0.5	2.5	4.9	11.8	22.2	31.3	39.4
500	0.2	1.0	2.0	4.9	9.5	13.9	18.1

$P_{e,scour}$, which is calculated according to the proposed framework, is defined as the exceedance probability of the actual scour depth exceeding the selected scour depth with consideration of uncertainties (FHWA 2023). MDOT calculated the deterministic scour elevation using HEC-18 equations as 514 ft for Q_{100} and 509 ft for Q_{500}. The research team also conducted the scour exceedance analysis using HEC-18 design equations, and the $P_{e,scour}$ of both floods was 19.8 and 6.9 percent, respectively. While the scour elevations increased for the decay function method, the $P_{e,scour}$ of the total pier scour depth for Q_{100} and Q_{500} were actually reduced from 19.8 and 6.9 percent, respectively, to 3.3 percent. The significant $P_{e,scour}$ improvement is mainly attributed to the consideration of soil erosion resistance of the clay layer when using the decay function method.

CONCLUSION

This paper proposed a probabilistic scour analysis approach—which used the Monte Carlo simulation, pier shear stress decay function, and soil resistance distribution—to assess the exceedance probability for incremental scour depths in bridge foundation design. The natural uncertainty, hydrological modeling uncertainty, hydraulic modeling uncertainty, equation uncertainty, and the uncertainty of critical shear stress of soil were considered to develop the hydraulic load and resistance distributions. Decay functions were used to relate presumed scour depths to bed shear stress. The Monte Carlo simulation was performed to realize the combination of uncertainties in load and resistance to obtain the results of $P_{e,scour}$ at various elevations at the foundation.

In the case study, 750,000 flow discharges were generated using a batch HEC-RAS computation that considered various statistical uncertainties in the flood event and a distribution of Manning *n* values. With the decay function equations and the computed approach shear stresses from the resulting Monte Carlo flow parameters, the distribution of decayed pier shear stress at incremental scour elevation was calculated. The exceedance probability of the total pier scour for a continuous depth can be determined by comparing the decayed shear stress against the soil resistance distribution at each depth. The $P_{e,scour}$ of the total fender scour reaching the clay layer at 530 ft was determined to be 3.3 percent in the 75-year bridge design life. For comparison, the probabilistic scour analysis was also performed by using the HEC-18 equation, in which the $P_{e,scour}$ of the design total fender scour depth was 19.8 and 6.9 percent for Q_{100} and Q_{500} floods, respectively. By using the decay function, which considered the resistance of the clay layer, the calculations lowered the $P_{e,scour}$ of total fender scour depth for Q_{100} and Q_{500} floods from 19.8 and 6.7 percent, respectively, to 3.3 percent.

This study result provides MDOT with a research tool to quantify a risk level in bridge foundation design. The result also demonstrated how NextScour, developed by FHWA, could significantly improve the accuracy of bridge scour estimates (FHWA 2023; Shan et al 2020). Future monitoring of the bridge site is recommended to verify the scour predictions after a flood event.

REFERENCES

AASHTO (American Association of State Highway and Transportation Officials). (2020) *AASHTO LRFD Bridge Design Specifications, 9th Edition.* Report No. LRFDBDS-9. AASHTO, Washington, DC.

Annandale, G. W. (2005) *Scour Technology: Mechanics and Engineering Practice.* McGraw-Hill Education, New York, NY.

Arneson, L., Zevenbergen L., Lagasse, P., and Clopper, P. (2012) *Hydraulic Engineering Circular No. 18, Evaluating Scour at Bridges, Fifth Edition.* Report No. FHWA-HIF-12-003. Federal Highway Administration, Washington, DC.

Beard, L. R. 1974. *Flood Flow Frequency Techniques.* Technical Report CRWR-119. Austin, TX: The University of Texas at Austin: Center for Research in Water Resources.

Doucet, A., Freitas, N., and Gordon, N. (2001) *Sequential Monte Carlo Methods in Practice.* Springer, New York, NY, https://doi.org/10.1007/978-1-4757-3437-9, last accessed March 21, 2023.

Efron, B., and Tibshirani, R. J. (1994) *An Introduction to the Bootstrap.* Chapman and Hall, New York, NY, https://doi.org/10.1201/9780429246593, last accessed March 21, 2023.

England, J. F., Cohn, T. A., Faber, B. A., Stedinger, J. R., Thomas, W. O., Veilleux, A. G., Kiang, J. E., and Mason, R. R. (2019) "Guidelines for Determining Flood Flow Frequency—Bulletin 17C." Chapter B5 in *US Geological Survey Techniques and Methods, Book 4.* U.S. Department of the Interior, Geological Survey, Reston VA.

FHWA. (2023) *NextScour Case Study: The Lafayette Avenue Bridge over the Saginaw River in Bay City, Michigan.* Report No. FHWA-HRT-23-104. Federal Highway Administration, Washington, DC.

Huang, C., Kerenyi, K., and Shen, J. (2019) "Incorporation of scour uncertainty to current AASHTO LRFD bridge design specifications." *Scour and Erosion IX: Proceedings of the 9th International Conference on Scour and Erosion (ICSE 2018).* Taipei, Taiwan. https://doi.org/10.1201/9780429020940, last accessed March 21, 2023.

Kerenyi, K., and Flora, K. (2019) "A Hybrid Approach to Forensic Study of Bridge Scour." *Proc. of the Institution of Civil Engineers: Forensic Engineering* 172(1), 27–38, https://doi.org/10.1680/jfoen.19.00001, last accessed March 21, 2023.

Lagasse, P. F., Ghosn, M., Johnson, P. A., Zevenbergen, L. W., and Clopper, P. E. (2013) *Reference Guide for Applying Risk and Reliability-based Approaches for Bridge Scour Prediction.* NCHRP Report No. 761. Transportation Research Board, Washington, DC.

Lee, G. C., Mohan, S., Huang, C., and Fard, B. N. (2013) *A Study of U.S. Bridge Failures (1980-2012).* Technical Report MCEER-13-0008. MCEER, Buffalo, NY.

Shan, H., Kerenyi, K., Pagenkopf, J., and Huang, C. (2020) "NextScour for Improving Bridge Scour Design in the United States." *Proc. of the Institution of Civil Engineers: Forensic Engineering,* 173(4), 121–129. https://doi.org/10.1680/jfoen.20.00017, last accessed March 21, 2023.